Modelling and experimental study of separators for co-solvent recovery in a supercritical extraction process

S. Camy, J.-S. Condoret *

Laboratoire de Génie Chimique, 5 rue Paulin Talabot, 31106 Toulouse Cedex 1, France

Abstract

Co-solvent recovery in supercritical extraction is addressed here through a theoretical description of the behaviour of a CO_2 + co-solvent mixture into a cascade of cyclonic separators, such as those existing in conventional fractionation processes based on depressurisation cascades. Conversely to the conventional simplified approach that considers a separator as a plain theoretical stage, our study proposes a dynamic modelling that accounts for the probable droplet entrainment by the light phase and the re-vaporisation phenomenon after the valve. Fractionation experiments of CO_2 + *n*-propyl alcohol mixtures were operated in a three-stage fractionation pilot, and experimental results are compared with simulation ones. The study demonstrates the relevance of our modelling, and points out the importance of entrainment effects, especially for low-pressure operated separators.

Keywords: Supercritical CO_2; Co-solvent; Cyclonic separators; Mechanical entrainment; Modelling

1. Introduction

The use of supercritical fluids, and especially carbon dioxide, as a solvent for applications of extraction (SFE) is now commonly spread, and concerns several domains, such as extraction of natural products for pharmaceuticals or food applications, or elimination of organic pollutants in cleaning applications [1–4]. However, the solvent power of carbon dioxide, often limited for extraction of polar molecules can be enhanced by small amount addition of an organic liquid, termed co-solvent or entrainer [2–5]. On a process point of view, addition of these compounds, often volatile, arises the problem, in addition to recovery of co-solvent non-polluted extracts, of their recovery and regeneration as in the case of extraction of aromatic compounds. The more conventional co-solvent recovery principle involves a depressurisation operated through a valve followed by a phase separator. Mechanical separation efficiency of this latter may take advantage of the well-known cyclone principle, such as in the apparatus developed by Separex [6]. However, this set-up was mainly designed in order to limit solid particle entrainment into the low-density phase (composed mostly of CO_2), and although they may be efficient for limiting liquid droplet entrainment, we know from our previous study that, in the case of desolubilisation of liquid compounds, this entrainment into CO_2 phase is actually occurring [7].

In this work, we have been interested in the theoretical description and modelling of these separators, and in the development of a model allowing the simulation of CO_2 + co-solvent mixture fractionation using a cascade of separators. In the field of supercritical extraction, the modelling of fractionation of the extracts has been the subject of very few studies. For example, Cesari et al. [8] have been interested in the model of a semi-batch process of extraction–separation, but they focused their work on the mathematical model describing the extraction step, of methanol from a methanol–water mixture by supercritical CO_2, as well as of citral from lemon oil. A similar study has been done by Benvenutti and Gironi [9], concerning the extraction of terpenic compounds from lemon essential

* Corresponding author. Present Address: LGC UMR CNRS5503, 5 rue Paulin Talabot, 31106 Toulouse Cedex 1, France. Tel.: +33 5 32 61 52 81; fax: +33 5 32 61 52 59.

E-mail address: JeanStephane.Condoret@ensiacet.fr (J.-S. Condoret).

Nomenclature

E	entrainment ratio
F	fluid flow rate (mol min^{-1})
$\hat{F}$	fluid quantity (mol)
$\hat{H}$	molar hold-up (mol)
$\hat{L}$	liquid quantity (mol)
$\hat{M}$	molar quantity submitted to the flash (mol)
P	pressure (MPa)
$\hat{S}$	externally collected withdrawal (mol)
T	temperature (K)
t	time (min)
v	molar volume (m^3 mol^{-1})
V	volume (m^3)
Vh	hold-up volume (m^3)
x	liquid mole fraction
y	fluid mole fraction
z	overall mole fraction

Subscripts

cont	contactor
i	component i
j	component j
sep	separator
t	time t

Superscripts

G	fluid phase
H	hold-up
IN	inlet
L	liquid phase
OUT	outlet
tot	total

Greek letters

Δt	time increment (min)
ω	molar vaporisation ratio

oil, but results representing the behaviour of the system in the post-extraction stage were not presented. In all these studies, the depressurisation step was simply described as a theoretical stage. In our previous study concerning dynamic modelling of a fractionation process [7], we attempted to propose a more suitable description, where establishment of thermodynamic equilibrium is located just after the depressurisation valve, and where a perfect segregation of phases occurs in the separator. However, this new model, although bringing some improvement, still does not provide a proper description of experimental results of fractionation. In this paper, we intend to propose a clear improvement for this description. The theoretical and experimental study will be based on the fractionation of a CO_2 + *n*-propyl alcohol model mixture.

2. Material and methods

2.1. Experimental pilot

Runs were carried out in a SEPAREX SF200 pilot (Separex Company, Nancy, France) represented in Fig. 1 and described elsewhere [7]. Briefly, this apparatus is composed of a 200-mL extractor autoclave that is used, as is the case here, as a simple liquid–fluid mixing chamber, for CO_2 and *n*-propyl alcohol, this latter being injected in the upstream tubing using a HPLC Pump (Gilson Model 8025). Indeed a metallic roll was placed inside the extractor, in order to reduce its volume from 200 to 20 mL. Mixing is ensured thanks to a magnetic stirrer. A cascade of three 15-mL cyclonic separators is connected to the mixing chamber outlet. Pressure in the mixing chamber is adjusted by a back-pressure regulator and, in each separator, by depressurisation valves.

Subcooled liquid CO_2 is pumped by a volumetric membrane pump (Milton Roy, maximum 5 kg/h), then heated until the desired temperature and continuously introduced into the mixing chamber. Experiments can be carried out in open-loop or closed-loop configuration, in which case, after condensation, CO_2 is recycled at the pump. Temperatures and pressures are controlled in each unit of the pilot, pressure being limited to 30 MPa and temperature around 333 K.

Before starting an experiment, the pilot is filled with CO_2 at bottle pressure (about 5.5 MPa) and air is flashed out. Then, CO_2 and liquid co-solvent are simultaneously pumped and heated into the contactor. Temperature of the mixture is adjusted thanks to heating fluid circulation in the jacket of the mixing chamber. At the outlet, the mixture undergoes three successive depressurisations. Each depressurisation stage is composed of a valve and a cyclonic separator with a heating jacket.

Temperature and pressure sensors are placed at each vessel outlet and measured values are recorded by a digital recorder (Memo-graph, Endress + Hauser) allowing monitoring of possible perturbations in the continuous operation.

Along the time, liquid phase accumulates at the bottom of each separator. As a consequence, each separator is entirely withdrawn at fixed intervals of time, and time necessary for this operation is measured. The flask receiving the collected liquid is rapidly immersed into ice in order to avoid any loss of co-solvent by evaporation, and, finally, the amount of collected liquid is weighed. Recording of temperatures and pressures is particularly useful to evaluate perturbations induced by the withdrawal of liquid samples.

2.2. Operating conditions

The mixture to be separated is about 5% co-solvent content and the CO_2 mass flow rate about 0.7 kg/h. Temperature and pressure in the contactor are set to, respectively, 328.15 K and 20 MPa, in order to be sure to keep the mixture monophasic before being separated.

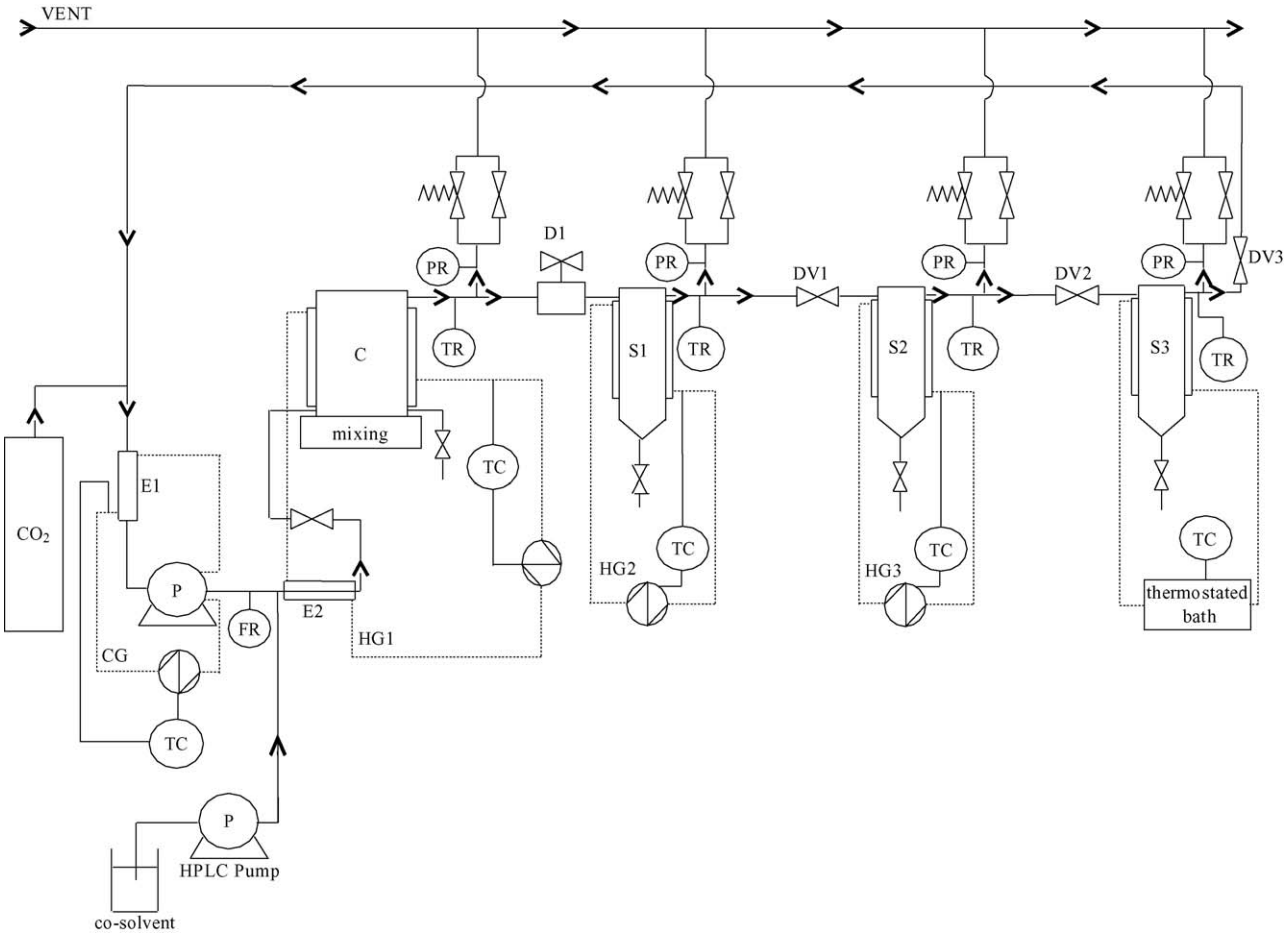

Fig. 1. Pilot SF200. C: mixing chamber; S1, S2, S3: separators; CG: cooling group; HG: heating group; PR: pressure recording; TC: temperature control; TR: temperature recording; D1: back-pressure regulator; DV1, DV2, DV3: depressurisation valves; E1: condenser; E2: evaporator.

2.3. Materials

CO_2 TP is supplied by air liquid and *n*-propyl alcohol by Scharlau (reagent grade, water content maximum 0.05%, AL 0437).

3. Modelling of separators

3.1. Theoretical description of separators

Our previous works [7] focused on the description of the contactor and separators of this kind of process. These works showed that if the contactor can be reasonably described as a theoretical stage of equilibrium, this is not true for cyclonic separator, and we proposed another description, based on the assumption that the mixture achieves thermodynamic equilibrium just after the depressurisation valve and that the resulting biphasic mixture undergoes perfect segregation of phases after leaving the separator. Although more suitable, this description failed in properly describing all experimental results, and led us to consider additional phenomena, such as mechanical entrainment of liquid droplets. This work led us to improve the description of separators following the scheme represented in Fig. 2:

- Firstly, the mixture (1) undergoes through the valve (A) an isenthalpic depressurisation up to the separator pressure, generating a biphasic mixture at temperature T_2.
- Then, this biphasic mixture (2) enters the separator and undergoes a distinct separation of phases (B), leading to a fluid (or vapor) mixture (3) and a liquid mixture (4).
- A usually small part of the liquid mixture (5) is added to the fluid (or vapor) phase as entrained droplets. The (C) unit represents this phenomenon of mechanical entrainment.

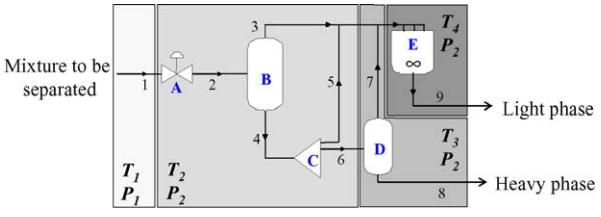

Fig. 2. Schematic representation of the depressurisation step.

- Then the residual liquid (6) heated in the separator at temperature T_3, is likely to re-vaporise dissolved CO_2 (unit D). So a part of the liquid mixture (6) becomes a fluid (or vapor), flux (7), mixes with the flows (3) and (5) (unit E), leads to the final exiting light phase (9).
- The final exiting heavy phase (8) is collected, and the final exiting light phase (9) is directed towards the next separator, or towards the exit of the process.

Temperatures and pressures of this depressurisation scheme are indicated in Fig. 2. Mixture to be separated enters the depressurisation valve at T_1 and P_1, and is depressurised to P_2. The adiabatic transformation brings the mixture to T_2. After being heated, temperature of residual liquid and vapor due to re-vaporisation is T_3. Resulting of adiabatic mixing of all flows leads to a temperature T_4 for the final exiting light phase (9).

For calculations, homogeneity of concentrations is assumed in each phase. The model takes into account the dynamics of the system, including the initial step of filling up of the contactor until steady-state is established. Each simulation of experimental run is based on particular operating conditions of the run. During an experiment, evolution of temperature and pressure is recorded. Time intervals and duration for removal of liquid samples are known and implemented in the simulation in order to take into account-induced perturbations.

As it is the case experimentally, at the beginning of a simulation, the system is considered filled with pressurised CO_2.

3.2. Mathematical modelling

In order to explain mass balance equations representing separator operation as described above, notations are clarified in Fig. 3.

As a convention, we choose to use superscripts L and G to indicate, respectively, the high-density liquid phase and the low-density fluid phase, and variables like "$\hat{Y}$" represent molar quantities. Equations are here presented for a system of two components, i.e. a mixture CO_2 + co-solvent.

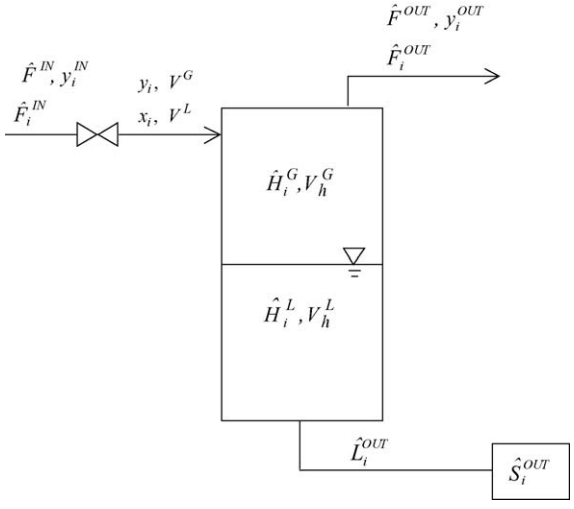

Fig. 3. Notations for the separator.

In the separator, the total amount of component i involved in the flash is calculated from entering flow rate:

$$\hat{M}_{i,t} = \hat{F}_{i,t}^{\mathrm{IN}}, \quad i = 1, 2 \tag{1}$$

Composition of this mixture is calculated with:

$$z_{i,t} = \frac{\hat{M}_{i,t}}{\sum_{i=1}^{2} \hat{M}_{i,t}}, \quad i = 1, 2 \tag{2}$$

Molar enthalpy of the flow before the depressurisation is calculated, thanks to BibPhy™ subroutine from the ProSim™ software package (PROSIM, S.A., France) giving properties of the flow after the depressurisation valve. This subroutine, solving the equation of equality of fugacities, gives the composition of phases (y_i and x_i), molar volumes of these phases, and vaporisation ratio ω of the mixture. Volumes V^{G} and V^{L} occupied by each phase can then be calculated:

$$V_t^{\mathrm{L}} = v_t^{\mathrm{L}} \cdot (1 - \bar{\omega}_t) \cdot \sum_{i=1}^{2} \hat{M}_{i,t} \tag{3}$$

$$V_t^{\mathrm{G}} = v_t^{\mathrm{G}} \cdot \bar{\omega}_t \cdot \sum_{i=1}^{2} \hat{M}_{i,t} \tag{4}$$

In the separator, the mixture undergoes a segregation of phases, so liquid hold-up is calculated by adding new liquid quantity to existing liquid hold-up, while taking into account the entrainment of a part of the liquid phase by the light phase:

$$\hat{H}_{i,t}^{\mathrm{L}} = \hat{H}_{i,t-\Delta t}^{\mathrm{L}} + (1 - E) \cdot V_t^{\mathrm{L}} \cdot \frac{x_{i,t}}{v_t^{\mathrm{L}}}, \quad i = 1, 2 \tag{5}$$

where E is the entrainment ratio. This liquid hold-up is then heated and a part of it is vaporised. Properties of the new liquid and light phases are obtained thanks to a flash calculation realised by BibPhy™ subroutine. The new hold-up after re-vaporisation can be expressed as follow:

$$\hat{H}_{i,t}^{\mathrm{L}} = V_t^{'\mathrm{L}} \cdot \frac{x_{i,t}^{'}}{v_t^{'\mathrm{L}}}, \quad i = 1, 2 \tag{6}$$

Hold-up volumes are then calculated by:

$$\mathrm{Vh}_t^{\mathrm{G}} = \mathrm{Vh}_{t-\Delta t}^{\mathrm{G}} + V_t^{\mathrm{G}} + V_t^{'\mathrm{G}} \tag{7}$$

$$\mathrm{Vh}_t^{\mathrm{L}} = V_t^{'\mathrm{L}} \tag{8}$$

$$\mathrm{Vh}_t^{\mathrm{tot}} = \mathrm{Vh}_t^{\mathrm{G}} + \mathrm{Vh}_t^{\mathrm{L}} \tag{9}$$

Two cases have to be considered, depending on whether withdrawal at the bottom of the separator is operated or not.

(i) The separator is withdrawn at t. In this case, amount of component i of the light phase leaving the top of the separator between t and $t + \Delta t$ is calculated as follow:

$$\hat{F}_{i,t+\Delta t}^{\mathrm{OUT}} = \frac{(\mathrm{Vh}_t^{\mathrm{G}} - V_{\mathrm{sep}})}{\mathrm{Vh}_t^{\mathrm{G}}} \cdot \left(\hat{H}_{i,t}^{\mathrm{G}} + V_t^{\mathrm{G}} \cdot \frac{y_{i,t}^{\mathrm{H}}}{v_t^{\mathrm{G}}} + V_t'^{\mathrm{G}} \cdot \frac{y_{i,t}'}{v_t'^{\mathrm{G}}} \right) + E \cdot V_t^{\mathrm{L}} \cdot \frac{x_{i,t}}{v_t^{\mathrm{L}}}, \quad i = 1, 2 \tag{10}$$

Amount of component i contained in the liquid phase and extracted from the separator is equal to:

$$\hat{L}_{i,t}^{\mathrm{OUT}} = \hat{H}_{i,t}^{\mathrm{L}}, \quad i = 1, 2 \tag{11}$$

Total amount of component i accumulated outside the separator is:

$$\hat{S}_{i,t}^{\mathrm{OUT}} = \hat{S}_{i,t-\Delta t}^{\mathrm{OUT}} + \hat{L}_{i,t}^{\mathrm{OUT}}, \quad i = 1, 2 \tag{12}$$

New liquid and vapor hold-up are, respectively:

$$\hat{H}_{i,t}^{\mathrm{L}} = 0, \quad i = 1, 2 \tag{13}$$

$$\hat{H}_{i,t}^{\mathrm{G}} = \frac{V_{\mathrm{sep}}}{\mathrm{Vh}_t^{\mathrm{G}}} \cdot \left(\hat{H}_{i,t}^{\mathrm{G}} + V_t^{\mathrm{G}} \cdot \frac{y_{i,t}^{\mathrm{H}}}{v_t^{\mathrm{G}}} \right), \quad i = 1, 2 \tag{14}$$

and new volumes of phases:

$$\mathrm{Vh}_t^{\mathrm{G}} = V_{\mathrm{sep}} \tag{15}$$

$$\mathrm{Vh}_t^{\mathrm{L}} = 0 \tag{16}$$

$$\mathrm{Vh}_t^{\mathrm{tot}} = \mathrm{Vh}_t^{\mathrm{G}} + \mathrm{Vh}_t^{\mathrm{L}} \tag{17}$$

(ii) The separator is not withdrawn. In this case, liquid accumulates inside the separator. Once again, several cases have to be considered. Indeed, in the case where liquid is not withdrawn, it may accumulate up to overflow towards the next separator. In that case, the amount of component i leaving the separator with the light phase can be expressed as follows:

$$\hat{F}_{i,t}^{\mathrm{OUT}} = \hat{H}_{i,t}^{\mathrm{G}} + V_t^{\mathrm{G}} \cdot \frac{y_{i,t}^{\mathrm{H}}}{v_t^{\mathrm{G}}} + V_t'^{\mathrm{G}} \cdot \frac{y_{i,t}'}{v_t'^{\mathrm{G}}} + (\mathrm{Vh}_t^{\mathrm{L}} - V_{\mathrm{sep}}) \cdot \frac{x_{i,t}'}{v_t'^{\mathrm{L}}}, \quad i = 1, 2 \tag{18}$$

and no liquid phase exits from the bottom of the separator:

$$\hat{L}_{i,t}^{\mathrm{OUT}} = 0, \quad i = 1, 2 \tag{19}$$

Liquid and vapor hold-up can be expressed by:

$$\hat{H}_{i,t}^{\mathrm{L}} = V_{\mathrm{sep}} \cdot \frac{x_{i,t}'}{v_t'^{\mathrm{L}}}, \quad i = 1, 2 \tag{20}$$

$$\hat{H}_{i,t}^{\mathrm{G}} = 0, \quad i = 1, 2 \tag{21}$$

New hold-up volumes are calculated with:

$$\mathrm{Vh}_t^{\mathrm{G}} = 0 \tag{22}$$

$$\mathrm{Vh}_t^{\mathrm{L}} = V_{\mathrm{sep}} \tag{23}$$

In the case where the volume of the liquid phase remains inferior to the volume of the separator, we have:

$$\hat{F}_{i,t}^{\mathrm{OUT}} = \frac{(\mathrm{Vh}_t - V_{\mathrm{sep}})}{\mathrm{Vh}_t^{\mathrm{G}}} \cdot \left(\hat{H}_{i,t}^{\mathrm{G}} + V_t^{\mathrm{G}} \cdot \frac{y_{i,t}^{\mathrm{H}}}{v_t^{\mathrm{G}}} + V_t'^{\mathrm{G}} \cdot \frac{y_{i,t}'}{v_t'^{\mathrm{G}}} \right) + E \cdot V_t^{\mathrm{L}} \cdot \frac{x_{i,t}}{v_t^{\mathrm{L}}}, \quad i = 1, 2 \tag{24}$$

Hold-up are expressed as follows:

$$\hat{H}_{i,t}^{\mathrm{L}} = \hat{H}_{i,t-\Delta t}^{\mathrm{L}}, \quad i = 1, 2 \tag{25}$$

$$\hat{H}_{i,t}^{\mathrm{G}} = \frac{\mathrm{Vh}_t^{\mathrm{G}} - (\mathrm{Vh}_t - V_{\mathrm{sep}})}{\mathrm{Vh}_t^{\mathrm{G}}} \cdot \left(\hat{H}_{i,t}^{\mathrm{G}} + V_t^{\mathrm{G}} \cdot \frac{y_{i,t}^{\mathrm{H}}}{v_t^{\mathrm{G}}} + V_t'^{\mathrm{G}} \cdot \frac{y_{i,t}'}{v_t'^{\mathrm{G}}} \right), \quad i = 1, 2 \tag{26}$$

A Fortran 77 program has been written in order to solve mass balances at each time increment, and, except for calculation of compositions of phases under thermodynamic equilibrium done thanks to BibPhy™ subroutine, no numerical algorithm is necessary. In that way, the system is considered as steady-state between two time increments. Our previous work [7] validated this "pseudo steady-state approximation".

4. Vapor–liquid equilibrium of the CO_2 + *n*-propyl alcohol mixture

As already mentioned, *n*-propyl alcohol (NPA) has been chosen as a model co-solvent in experiments and simulations. The rather high boiling point of this compound under atmospheric conditions minimizes losses at the withdrawing step and furthermore experimental vapor–liquid equilibrium data for the CO_2 + NPA mixture can be easily found in literature.

Liquid–vapor equilibria of the mixture have been calculated using the Soave, Redlich and Kwong [12] equation of state with the MHV-2 mixing rules proposed by Michelsen [13]. The UNIQUAC [14] activity coefficient model has been chosen to determine the value of the free excess Gibbs energy needed in the calculation of the mixture parameters. In this

Table 1
Binary interaction parameters for the CO_2–NPA system

$A_{\mathrm{CO_2\text{-}NPA}}$ (cal mol^{-1})	−105.031
$A_{\mathrm{NPA\text{-}CO_2}}$ (cal mol^{-1})	669.11

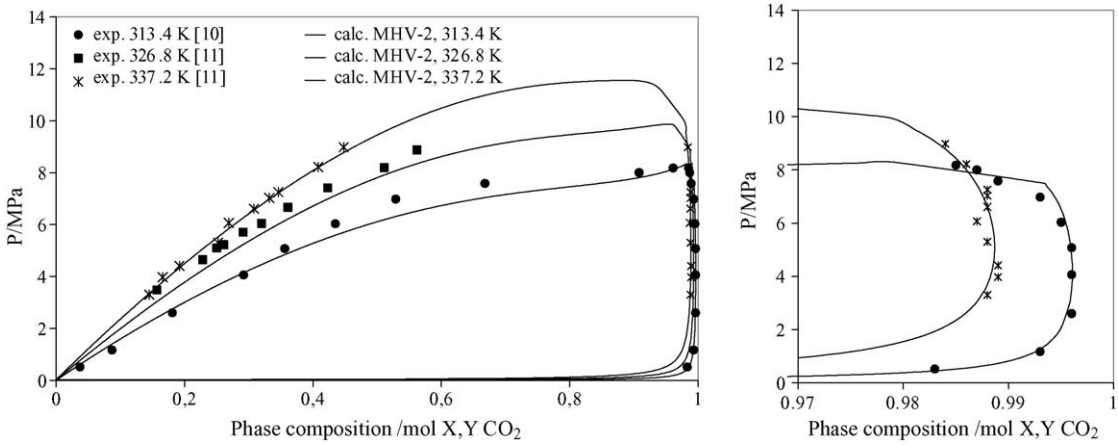

Fig. 4. Experimental and calculated P–x,y phase equilibrium for the CO_2 + NPA mixture at different temperatures.

case, it is necessary to know the value of binary interaction parameters A_{ij} and A_{ji} for the CO_2 + NPA mixture. These parameters have been obtained by fitting experimental results of the literature [10,11] thanks to the commercial software ProReg™ (PROSIM, S.A., France), and are listed in Table 1. A comparison of experimental and calculated vapor–liquid equilibria is represented in Fig. 4. As can be seen from this figure, experimental points are quite well fitted by the model. Simulations of the whole process of fractionation are performed on the basis of this thermodynamic model to represent phase equilibria in each point of the process.

5. Results and discussion

5.1. Comparison of experimental and calculated results

For each experiment, carried out on the experimental pilot described above, liquid accumulated in the bottom of each separator is regularly collected following a rigorous procedure where the withdrawal valve at bottom of the separator is carefully opened to collect the liquid avoiding escape of the gas. When no liquid is flowing any longer, the valve is closed. Average time for this operation is about 30 s. Amount of each sample is weighed and compared to calculated one. Simulations are performed taking into account real experimental conditions, i.e. pressure and temperature evolution recorded during the whole process, as well as frequency and duration of each withdrawal. Experiments last about 2 h and intervals between manual withdrawals vary between 5 to 10 min for the 1st separator, 7 to 15 min for the second one, and 20 min for the last one, depending on operating conditions. Indeed, the 1st separator is the most rapidly filled, and it is necessary to take care to avoid its complete filling up.

As mentioned before, the mixing chamber is maintained at about 20 MPa and 328.15 K for all experiments in order to be sure the mixture is monophasic before entering the first depressurisation stage. Moreover, the pressure of the first depressurisation stage has to be kept under 8 MPa to be sure that the depressurisation actually leads to a biphasic mixture.

Simulations are first performed using an entrainment ratio of 5% for the three separators. In the following, calculations named "Sim1" refer to this case. Moreover, we have tried to find entrainment ratio values allowing better matching of the experimental results, and this simulation is named "Sim2". We choose to present experimental and calculated results in terms of instantaneous NPA amount collected at the bottom of each separator and cumulative NPA amount, as a function of time. Moreover, amounts collected in the last separator being very weak, we decided to present only results obtained for the 1st and the 2nd separator. Experimental conditions of runs are described in Table 2 and Figs. 5 and 7, and comparison of experimental data and results of simulations are shown in Figs. 6 and 8.

From the recordings of temperatures and pressures, we can notice that pressure and temperature in the contactor are very stable, and this is mainly due to the efficiency of the back-pressure regulator at the mixing chamber outlet. Furthermore, great disturbance in this part of the process are not very probable. On the contrary, we can observe significant pressure and temperature drops for the separators, and this coincides with the collection of accumulated liquid. For the two experiments, deepest pressure drops (often greater than 1 MPa) occur in the 2nd separator, while temperature drops

Table 2
Experimental conditions for the runs

Run	D_{NPA} (kg h^{-1})	D_{CO2} (kg h^{-1})	X_{NPA} (wt)	$P_{C\ mean}$ (MPa)	$P_{S1\ mean}$ (MPa)	$P_{S2\ mean}$ (MPa)	$P_{S3\ mean}$ (MPa)	$T_{C\ mean}$ (K)	$T_{S1\ mean}$ (K)	$T_{S2\ mean}$ (K)	$T_{S3\ mean}$ (K)
1	0.0271	0.6912	0.0377	20.0	7.6	4.3	0.9	323.15	311.15	300.15	297.15
2	0.0235	0.7008	0.0324	19.9	6.9	4.8	0.9	323.15	308.15	306.15	294.15

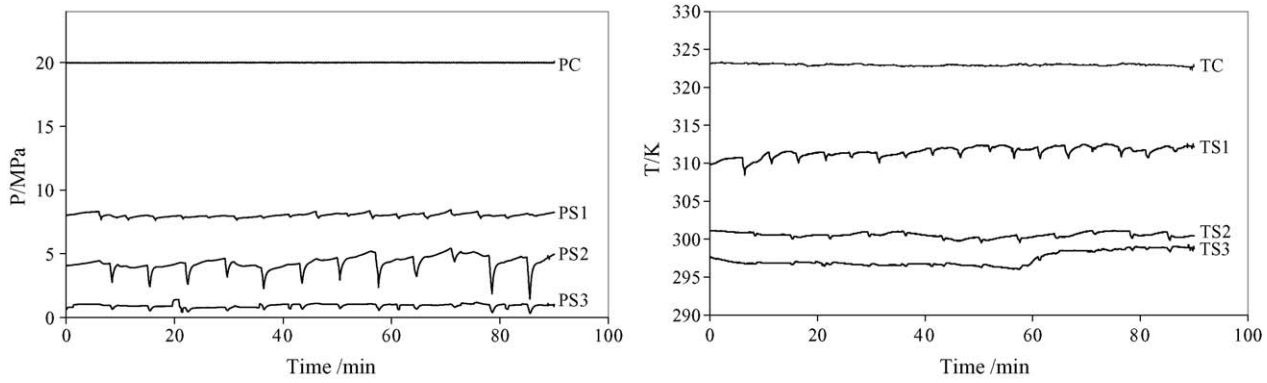

Fig. 5. Recordings of pressure and temperature evolution for the experimental run no. 1.

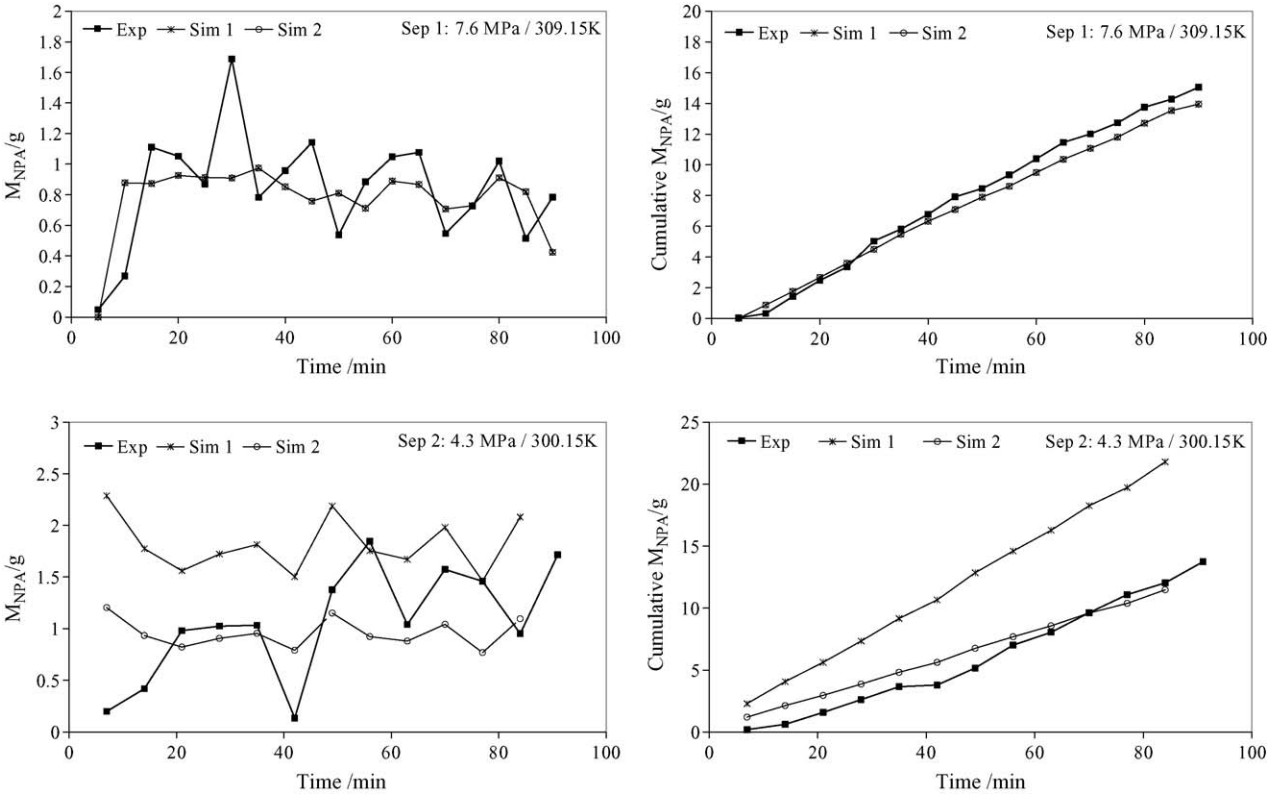

Fig. 6. Comparison of instantaneous and cumulative amount of NPA collected experimentally and calculated for run no. 1.

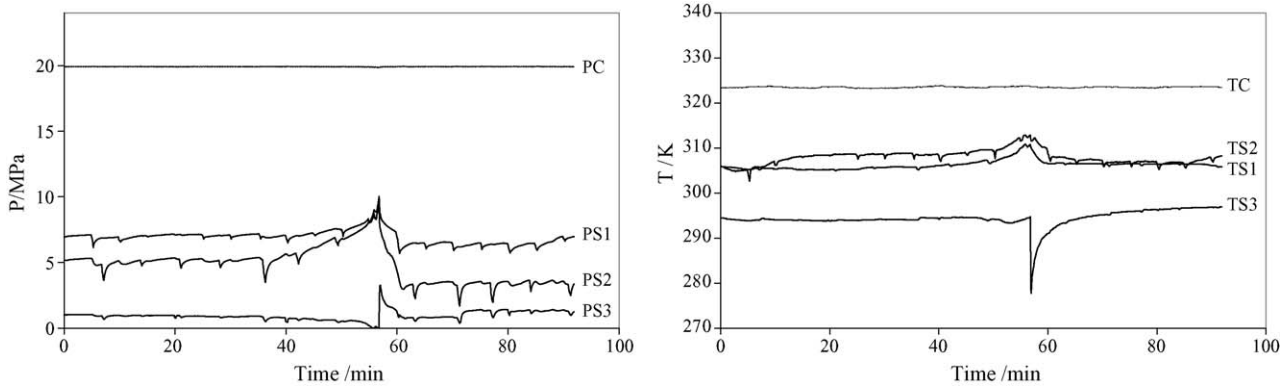

Fig. 7. Recordings of pressure and temperature evolution for the experimental run no. 2.

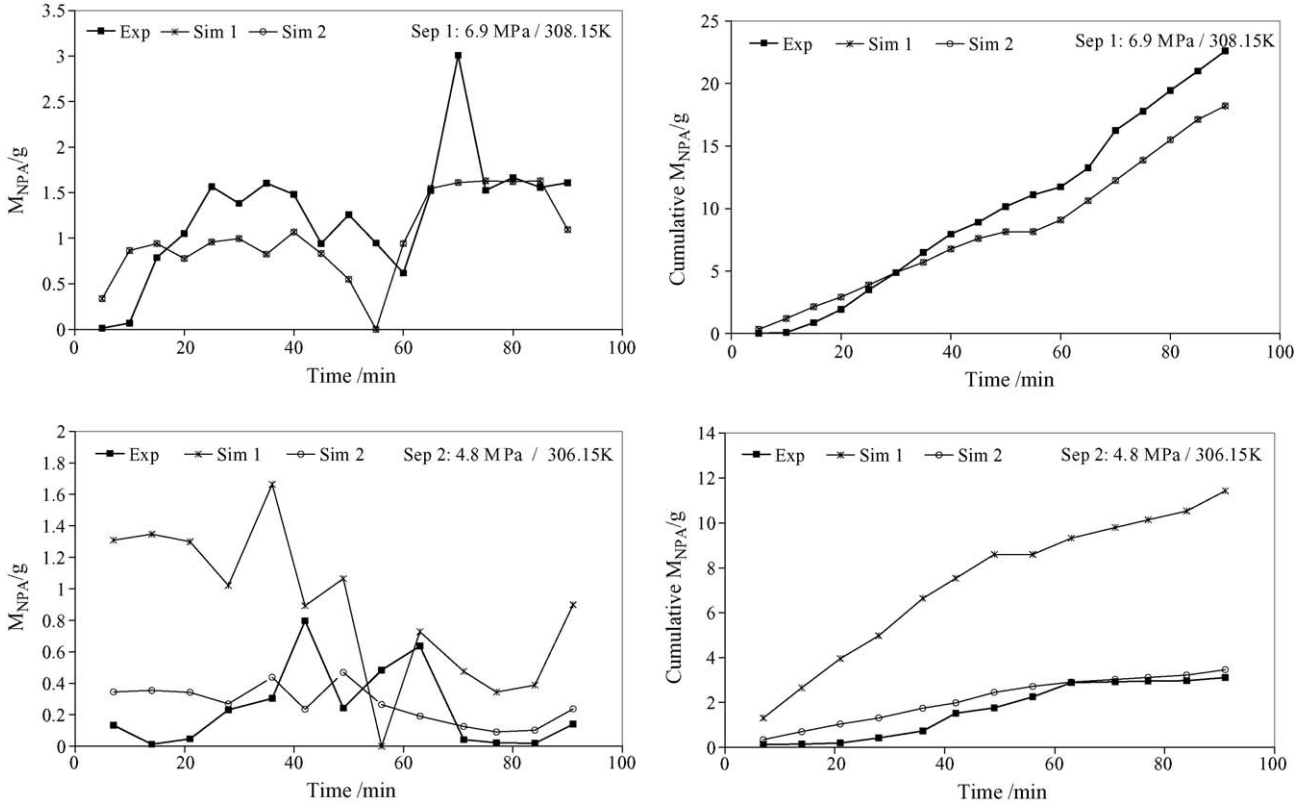

Fig. 8. Comparison of instantaneous and cumulative amount of NPA collected experimentally and calculated for run no. 2.

are more important in the first one, although they remain quite weak (about 1 K) compared to pressure drops. Concerning run no. 2, at about 57 min, recording shows a positive peak of pressure in separators 1 and 2, and a pressure drop in separator 3. In the same way, temperatures of separators 1 and 2 increase at this moment and we observe a large temperature drop for the last separator. We have related these sharp variations to the freezing of the depressurisation valve between separators 2 and 3 observed at this time. This freezing led to solidification of CO_2 through the valve and as a consequence to a blocking of the valve, inducing an increase of upstream pressures and a decrease of pressure of the last separator. The situation was set back to normal simply by manual defreezing using a hot-air blower.

These recordings evidence clearly perturbations when bottoms of separators are opened to recover liquid. The pressure drop leads to great changes in the mixture properties, such as density, where the mixture is not far from the monophasic zone. For this reason, it seems to be very important to take this point in consideration for the design of withdrawal set-up. Moreover, in order to perform as reliable as possible simulations, we think quite important to take variations of operating conditions into account. As a consequence, our simulation programs have been written to be able to read experimental values of temperature and pressure in order to interpolate in real time values of these conditions. Nevertheless, it is important to point out that perturbations are particularly significant in small volume separators, such as those of our experimental pilot. Liquid recovery from separators may be a less critical operation when operated on industrial scale pilots.

Experimental results concerning the 1st separator show that, after a first phase of steady-state establishment, amount of collected NPA oscillates around an average value. This is due to the regular frequency of withdrawals and to their quasi-constant duration. Consequently, accumulated amount increases quasi-linearly. However, some values deviate more or less from this average value, because withdrawals, even done with a rigorous procedure, are manually operated, and collected amounts are ineluctably related to the operator skills. This "technical" difficulty does not seem avoidable as far as the recovery of accumulated liquid is not performed thanks to an automatic device. Moreover, we have seen that, because of withdrawals, operating conditions are not constant, and this has an influence on the thermodynamic behaviour of the mixture and thus on the liquid condensation.

When comparing simulation to experiments, we can say that results concerning the 1st separator show a suitable adequacy between experimental and calculated results. Tendencies are correctly described by the model and the computed NPA collected amount are in the same range. Because simulations take temperatures and pressures variations into account, results from calculations can account for some irregular oscillations of instantaneous NPA amount, although intensity of these oscillations is smoothed compared to experimental ones. Concerning the cumulated collected amounts, results for run no. 1 show that calculated rate of

condensation matches very well the experimental values. Difference between these experimental and calculated values is more important for run no. 2. Indeed, for this run, we saw that pressure increase occurred because of the freezing of the CO_2 into the valve. Moreover, we noticed that, first depressurisation should be performed at pressure less than 8 MPa in order to cause a condensation of a part of the mixture. As a consequence, for this period of the run where pressure in the 1st separator was temporarily higher, simulations indicate that no liquid should be formed in the 1st separator. However, experimental results show a decrease but not a disappearance of the condensed amount. Explanation might come from the thermodynamic part of the modelling. Indeed, the mixture oscillates close to its bubble line, and, as can be seen on the equilibrium curve of Fig. 4, in this case, thermodynamic modelling is not very accurate.

5.2. *Effect of the entrainment ratio E*

As mentioned before, simulations were first carried out with an entrainment ratio equal to 5 wt.% for the 1st separator, and this value had seemed to be in accordance with experimental results. This has been moreover confirmed by our other experiments (not presented here). Considering available accuracy of our experimental procedure, we consider calculations for the 1st separator as very satisfactory.

Results concerning the 2nd separator reveal a global tendency: calculations performed with a 5 wt.% entrainment ratio tend to overestimate NPA collected amounts. As a consequence, we adjust by trials and errors the value of the entrainment ratio of this separator until we found good matching between experimental and calculated results. We can see in Table 3 that adjusted entrainment ratio is now very high (50–75%). However, from these experiments (and from others not presented here), it was not possible to establish a direct link between operating conditions and entrainment ratio. Same result was observed for the 3rd separator too, where calculated entrainment ratios reach 90% when pressure is around 1 MPa. In a first approach, this result may be surprising because, conventionally, low-density difference between light and heavy phase, as in the 1st separator, is considered as unfavourable for phase separation. Here, on the contrary, high-density difference, as in the 2nd and the 3rd separator, gave surprisingly worse efficiency than in the 1st separator. Special care has been taken to find possible leaks in the separator, because they cause the modelling to achieve important entrainment ratios, but no leaks were found. One explanation may be found in the fact that, in the 1st separator, most part of the NPA is condensed, and the presence of this important liquid phase volume may help significantly the coalescence of liquid droplets, so reducing entrainment phenomenon. On the contrary, very small quantity of liquid is formed after the 3rd depressurisation valve, and this may be a reason for the important entrainment ratio calculated for the 3rd separator. On a practical point of view, high values of the entrainment ratio must be moderated by the fact that it applies to small fluxes. All these hypotheses should be the subject of a thorough study concerning hydrodynamics inside the separator, which could reveal information on phenomenon of liquid droplet formation through the depressurisation valve, size distribution of these droplets in a supercritical fluid, and coalescence of these droplets inside the separator. As a consequence, we think that entrainment ratio is obviously related to hydrodynamics inside the separator, but also to the physico-chemical properties of phases in presence as well as their respective quantities. As a conclusion, provided high entrainment ratios are admitted, fitted calculations give satisfactory results, and represent correctly orders of magnitudes and general tendencies of the curves.

Table 3
Entrainment ratios used for simulations

Run	Simulation	E_{S1} (wt.%)	E_{S2} (wt.%)
1	Sim1	5	5
	Sim2	5	50
2	Sim1	5	5
	Sim2	5	75

5.3. *Comments on mass balances*

Table 4 presents mass balances for runs no. 1 and 2 and 6 other runs, the results of which are not presented

Table 4
Experimental and calculated NPA recovery ratio

Run	$\%_{recov}$ Separator 1	$\%_{recov}$ Separator 2	$\%_{recov}$ Separator 3	$\%_{recov}$ Total
1				
Exp	41.5	36.3	5.7	83.5
Sim	36.9	29.4	0.1	66.4
2				
Exp	74.3	11.8	10.3	96.4
Sim	53.3	9.2	6.0	68.5
3				
Exp	50.7	18.2	1.1	70.0
Sim	36.8	18.1	4.3	59.2
4				
Exp	6.4	66.2	5.0	77.6
Sim	3.9	45.5	4.9	54.3
5				
Exp	21.8	38.8	11.4	72.0
Sim	21.9	34.1	8.7	64.7
6				
Exp	29.8	52.2	7.0	89.0
Sim	28.7	48.6	6.6	83.9
7				
Exp	29.5	40.0	13.9	83.4
Sim	34.5	44.6	13.6	92.7
8				
Exp	87.1	4.1	0.8	92.0
Sim	87.5	4.0	1.2	92.7

in details in this study, and only NPA experimental and calculated recovery ratios for each separator are given. Results of simulations presented in this table have been obtained from simulations with adjusted individual entrainment ratios for the 2nd and the 3rd separator. Mass balances are done between $t = 20$ and 80 min, in order to get rid of the influence of a hold-up in the dead volume of the pilot.

We can note in Table 4 that, although for some deviations exist between experimental and calculated NPA recovery ratios, orders of magnitude are essentially respected by simulations. A mean deviation of about 20% can be calculated on total recovery ratios. Our results show that, with operating conditions applied in this study, NPA is not totally recovered in the separators. However, total recovery ratios remain high, from 70 to 96%, which means that co-solvent recovery can be still envisaged with this type of simple process equipped with cyclonic separators.

6. Conclusion

This paper has addressed the problem of co-solvent recovery in supercritical extraction through a theoretical description of the behaviour of a CO_2 + co-solvent mixture into a cascade of cyclonic separators, such as those existing on conventional fractionation processes based on depressurisation cascades. We have brought here an improvement to the conventional over simplified description of such separators, usually considered like plain theoretical stages. Here, the depressurisation stage is described as a unit comprising the depressurisation valve, from where the mixture exits under thermodynamic equilibrium, and the cyclonic separator, where the biphasic mixture undergoes segregation of phases accompanied by an entrainment of liquid droplets by the light phase, and partial re-vaporisation of the entering liquid phase. A simulation program based on this model and taking into account dynamics of the system was written and validated using fractionation experiments performed with a three-stage fractionation pilot. With a CO_2 + *n*-propyl alcohol test mixture, this latter playing role of a co-solvant, comparison of experimental and calculated results have shown the relevance of our modelling, although accuracy of results were handicapped by the small size of the pilot.

This study pointed out the importance of the correct representation of liquid–vapor equilibria of the mixture, in particular when fractionation takes place near the critical zone of the mixture. A good representation of the thermodynamics of these systems is still a prerequisite for study of processes involving supercritical fluids.

An other interesting result is that non-negligible entrainment effect exists. This phenomenon, introduced in the model using the parameter "entrainment ratio", was found here dependent of the rank of separator in the cascade, because different operating conditions led to different intern hydrodynamics of the separators. A contra intuitive result was that entrainment was higher in the liquid–vapor separation zone, instead than in the liquid–fluid zone. Provided the good choice of the value of this entrainment parameter, we consider that our model offers a proper description of phenomena occurring inside a separator. Nevertheless, only a deeper study, using the tools of computational fluid dynamics could bring rational determination of the parameters. Fortunately, on an industrial scale, importance of the entrainment parameter is likely to be lowered because of the bigger size of the separators, and our model, fed with rather small value of the entrainment ratio, would remain a valuable tool to determine optimum operating conditions of an industrial unit.

Acknowledgment

This work was supported by the Research Center of L'AIR LIQUIDE Company in the framework of a scientific collaboration.

References

[1] V. Librando, O. Hutzinger, G. Tringali, M. Aresta, Supercritical fluid extraction of polycyclic aromatic hydrocarbons from marine sediments and soil samples, Chemosphere 54 (2004) 1189–1197.
[2] F. Bordet, T. Chartier, J.-F. Baumard, The use of co-solvents in supercritical debinding of ceramics, J. Eur. Ceram. Soc. 22 (2002) 1067–1072.
[3] M. Zougagh, M. Valcarcel, A. Rios, Supercritical fluid extraction: a critical review of its analytical usefulness, Trends Anal. Chem. 23 (2004) 1–7.
[4] C. Xu, D.W. Minsek, J.F. Roeder, M.B. Korzenski, T.H. Baum, Supercritical Fluid Cleaning of Semiconductor Substrates, US Patent 2003125225 (2003).
[5] K.C. Zancan, M.O.M. Marques, A.J. Petenate, M.A.A. Meireles, Extraction of ginger (*Zingiber officinale* Roscoe) oleoresin with CO_2 and co-solvents: a study of the antioxidant action of the extracts, J. Supercrit. Fluids 24 (2002) 57–76.
[6] M. Perrut, Device for carrying out extraction–separation–cracking processes by supercritical fluids, US Patent 4724087 (1988).
[7] S. Camy, J.-S. Condoret, Dynamic modelling of a fractionation process for a liquid mixture using supercritical carbon dioxide, Chem. Eng. Proc. 40 (2001) 499–509.
[8] G. Cesari, M. Fermeglia, I. Kikic, M. Policastro, A computer program for the dynamic simulation of a semi-batch supercritical fluid extraction process, Comput. Chem. Eng. 13 (1989) 1175–1181.
[9] F. Benvenutti, F. Gironi, Dynamic simulation of a semicontinuous extraction process using supercritical solvent, in: Proceedings of the fifth Conference on Supercritical Fluids and their Applications, Garda, 1999.
[10] K. Suzuki, H. Sue, M. Itou, R.L. Smith, H. Inomata, Isothermal vapor–liquid equilibrium data for binary systems at high pressures: carbon dioxide–methanol, carbon dioxide–ethanol, carbon dioxide–1-propanol, methane-ethanol, methane-1-propanol, ethane-ethanol, and ethane-1-propanol systems, J. Chem. Eng. Data 35 (1990) 63–66.
[11] V. Vandana, A.S. Teja, Vapor–liquid equilibria in the carbon dioxide + 1-propanol system, J. Chem. Eng. Data 40 (1995) 459–461.

[12] G.S. Soave, Equilibrium constants from a modified Redlich-Kwong equation of state, Chem. Eng. Sci. 27 (1972) 1197–1203.
[13] M.L. Michelsen, A modified Huron–Vidal mixing rule for cubic equations of state, Fluid Phase Equilibria 60 (1990) 213–219.
[14] D.S. Abrams, J.M. Prausnitz, Statistical thermodynamics of liquid mixtures: a new expression for the excess Gibbs energy of partly or complete miscible systems, AIChE J. 21 (1975) 116–128.